

Behavior of bolted angle connections subjected to combined shear force and moment

Akbar Pirmoz^{a,*}, Amir Saedi Daryan^a, Ahad Mazaheri^b, Hajar Ebrahim Darbandi^c

^a Civil Engineering Department of K.N. Toosi University of Technology, Tehran, Iran

^b Civil Engineering Department of Islamic Azad University of Urmia, Urmia, Iran

^c Master of Architecture, University of Tehran, Iran

Received 8 January 2007; accepted 23 September 2007

Abstract

In this paper, the effect of web angle dimensions on moment–rotation behavior of bolted top and seat angle connections, with double web angles is studied. Several 3D parametric finite element (FE) models are presented in this study whose geometrical and mechanical properties are used as parameters. In these models, all of the connection components, such as beam, column, angles and bolts are modeled using solid elements. The effect of interactions between components, such as slippage of bolts and frictional forces, are modeled using a surface contact algorithm. To evaluate the behavior of connection more precisely, bolt pretensioning force is applied on bolt shanks as the first load case. The results of this numerical modeling are compared with the results of experimental works done by other researchers and good agreement was observed. To study the influence of shear force on behavior of these connections, several models were analyzed using different values of shear force. The effect of important parameters, especially the effect of web angle dimension, is studied then. An equation is proposed to determine the reduction factor for initial rotational stiffness of connection using connection initial rotational stiffness, yield moment, the expected shear force and web angle dimension. The proposed equation is compared with other existing formulations and it was observed that the proposed model is a better estimator of connection behavior.

© 2007 Elsevier Ltd. All rights reserved.

Keywords: Steel structures; Bolted angle connection; Finite element modeling; Web angles; Shear force; Connection stiffness

1. Introduction

The Northridge earthquake (1994) and the Hyogoken-Nanbu (Kobe 1995) earthquake caused severe damage in welded moment connections of steel frames [1,2]. Since then, many alternative types of connections have been suggested by researchers, such as bolted top and seat angle connections.

These types of connections are categorized as semi-rigid connections [3] which have not the brittle fracture behavior of corresponding welded connections. On the other hand, these connections have deformable failure patterns and relatively large energy dissipation capacity.

An analytical study was done on 5 and 10 storey steel buildings [4]. Interior hybrid semi-rigid frames and interior welded moment frames of these buildings had different strengths and stiffness. The buildings were subjected to three

earthquake excitations. The results showed that interior semi-rigid frames can provide less storey shear, less column moment and high seismic performance for a structure.

Analysis and design of a semi-rigid frame needs a clear understanding of moment–rotation behavior of its connections. Lots of studies have been done all over the world to estimate the moment–rotation behavior of bolted top and seat angle connections. Azizinamini et al. [5] have experimentally studied the behavior of such connections under monotonic and cyclic loadings. The results of these experiments provide a rigorous reference which is used by later researchers to verify their proposed methods. Shen and Astaneh-Asl [6] have experimentally tested the behavior of bolted angle connections and the failure modes and deformation patterns.

Recently, numerical modeling, especially the finite element method, is used to investigate the behavior of this type of connection. Citipitioglu et al. [7] have studied the influence of bolt pretensioning and friction coefficient of the adjacent

* Corresponding author.

E-mail address: a.pirmoz@gmail.com (A. Pirmoz).

surfaces on the behavior of such connections in detail using the FE (Finite Element) method. In these models, all connection components were modeled using brick elements, while the effect of adjacent surfaces was considered. Kishi et al. [8] have studied the behavior of these connections using the finite element method. They have evaluated the applicability of a three-parameter relation (proposed by Kishi and Chen) for estimating the behavior of semi-rigid connections. Their FE models included the material nonlinearity for all components and the value of 0.1 was assumed for the friction coefficient. This coefficient is one-third of the usual value (0.33) proposed in the literatures for class “A” types of steel surfaces. Ahmed et al. [9] studied the prying action of the bolts in the top and seat angle connections using the FE method. This study showed that prying force depends on bolt diameter, gage distance and top and seat angle thickness. It also showed that the bolt’s pretensioning increases the initial stiffness of connection. Pirmoz has studied the influence of beam dimensions and friction coefficients of connection components on the moment–rotation behavior of bolted angle connections under monotonic and cyclic loading. He also studied the applicability of the FE method in studying the connection behavior and dynamic parameters of semi-rigid frames [10]. In this study, deterioration of frictional surfaces is considered. Results of these studies showed that in spite of the flexibility of the FE method to evaluate the behavior of bolted connections under cyclic loads, the method is very time consuming. Danesh and Pirmoz [11] have studied the effect of beam length on moment–rotation behavior of top-seat angle with double web angles using the FE method. In this study, the applicability of this type of connection in steel frames as a lateral resisting system against severe earthquakes is also studied.

Using the FE method to study the behavior of bolted angle connections, despite its accuracy, is a time consuming and expensive method. Thus many researchers proposed multi-linear and bilinear formulations to estimate the behavior of such connections. Shen and Astaneh-Asl [12] proposed a hysteretic model for bolted angle connection based on fiber element formulation. They categorized connections based on deformation patterns and failure modes and proposed some equations with regard to their behavior. Danesh [13] has proposed a bilinear formulation to estimate the behavior of bolted top and seat angle connections based on plastic hinges made in top angle and considering shear deformation effect on the capacity of the top angle leg.

In the last decade, artificial intelligence techniques have emerged as a powerful tool that could be used to replace time consuming procedures in many scientific or engineering applications. Abdalla and Stavroulakis [14] have used neural networks to predict the global moment–rotation curve of single web angle beam-to-column joints. De Lima et al. [15] employed neural networks for assessment of beam-to-column joints. Pirmoz and Gholizadeh [16] have used neural networks to predict global moment–rotation behavior of top and seat bolted angle connections with double web angles.

All the proposed models have a good accuracy for the case of pure bending or low zero shear force in connection. But

in most of the cases, beams and connections of a practical frame sustain gravitational loads and as a result, an inherent shear force due to these loads, since this type of connection is mainly designed to sustain gravitational loads. Another case in which high shear force exists in connections is the link to column connections in eccentrically braced frames (EBF). In such systems, lateral resistance of the frame is satisfied by braces and relatively short beams named a link beam and their inelastic action is primarily limited to these ductile links. Link beams and their connection to the column sustain high shear loads due to link–brace interactions in an earthquake. Some of the typical EBFs are arranged to have one end of the link connected to a column and this connection may be a pinned or semi-rigid bolted angle connection [17]. The connection stiffness change, caused by link shear force, must be considered in analyzing EBF to estimate frame behavior more accurately.

The behavior of double angle connections which are welded to the column web and bolted to the beam web was studied under shear, tension and the combination of these loads, using the finite element method and also experimental studies done by earlier researchers [18–20]. Thickness of web angles and bolt gage distance were used as parameters. The study showed that these types of connections behave like simple shear connections under a combination of axial and shear force.

In [21] the influence of shear force on initial stiffness of top-seat angle connections with double web angles subjected to shear force is studied using the FE method and an equation is proposed in terms of the connection initial stiffness, yield moment and expected shear force by curve fitting. This formulation does not consider directly the effect of some parameters such as web angle dimensions and bolt diameters, so the method has relatively low accuracy.

It is well known that the design of structures is a trial and error process, especially in systems with high redundancy, Also it is shown later that the moment resistance of connection is not affected considerably by applied shear force. So, only the influence of shear force on initial stiffness of bolted top-seat angle connections which affects the properties of the structure (such as its period or storey drifts computed by elastic analysis) is studied in this paper.

For this purpose a parametric FE model is created and verified by the results of an experimental study done by Azizinamini. The effect of shear force on connection behavior is evaluated by a number of models using shear force as variable. According to the rate of stiffness reduction due to increasing the shear force, an equation is proposed to determine the reduction factor of initial stiffness for such connections. The effect of web angle on overall response of connection is also studied and an increase in connection moment capacity is achieved.

2. Connection modeling

The finite element models used for this study were created according to the specimens used in the experimental work of Azizinamini [5]. The objective of these tests was to investigate the influence of different geometric properties of connections

Table 1
Geometrical properties of models used by Azizinamini

Specimen number	Bolt diameter (mm)	Column section	Beam section	Top and seat angle				Web angle	
				Angle	Length (mm)	Gage (g) (mm)	Bolt spacing (p) (mm)	Angle	Length (mm)
14S1	19.1	W12 × 96	W14 × 38	L6 × 4 × 3/8	20.32	6.35	13.97	2L4 × 3–1/2 × 1/4	215.9
14S2	19.1	W12 × 96	W14 × 38	L6 × 4 × 1/2	20.32	6.35	13.97	2L4 × 3–1/2 × 1/4	215.9
14S3	19.1	W12 × 96	W14 × 38	L6 × 4 × 3/8	20.32	6.35	13.97	2L4 × 3–1/2 × 1/4	139.7
14S4	19.1	W12 × 96	W14 × 38	L6 × 4 × 3/8	20.32	6.35	13.97	2L4 × 3–1/2 × 3/8	215.9
14S5	22.3	W12 × 96	W14 × 38	L6 × 4 × 3/8	20.32	6.35	13.97	2L4 × 3–1/2 × 1/4	215.9
14S6	22.3	W12 × 96	W14 × 38	L6 × 4 × 1/2	20.32	6.35	13.97	2L4 × 3–1/2 × 1/4	215.9
14S8	22.3	W12 × 96	W14 × 38	L6 × 4 × 5/8	20.32	6.35	13.97	2L4 × 3–1/2 × 1/4	215.9
8S1	19.1	W12 × 58	W8 × 21	L6 × 3–1/2 × 5/16	15.24	5.08	8.89	2L4 × 3–1/2 × 1/4	139.7
8S2	19.1	W12 × 58	W8 × 21	L6 × 3–1/2 × 3/8	15.24	5.08	8.89	2L4 × 3–1/2 × 1/4	139.7
8S3	19.1	W12 × 58	W8 × 21	L6 × 3–1/2 × 5/16	20.32	5.08	8.89	2L4 × 3–1/2 × 1/4	139.7
8S4	19.1	W12 × 58	W8 × 21	L6 × 6 × 3/8	15.24	13.72	8.89	2L4 × 3–1/2 × 1/4	139.7
8S5	19.1	W12 × 58	W8 × 21	L6 × 4 × 3/8	20.32	6.35	8.89	2L4 × 3–1/2 × 1/4	139.7
8S6	19.1	W12 × 58	W8 × 21	L6 × 4 × 5/16	15.24	6.35	8.89	2L4 × 3–1/2 × 1/4	139.7
8S7	19.1	W12 × 58	W8 × 21	L6 × 4 × 3/8	15.24	6.35	8.89	2L4 × 3–1/2 × 1/4	139.7
8S8	22.3	W12 × 58	W8 × 21	L6 × 3–1/2 × 5/16	15.24	5.08	8.89	2L4 × 3–1/2 × 1/4	139.7
8S9	22.3	W12 × 58	W8 × 21	L6 × 3–1/2 × 3/16	15.24	5.08	8.89	2L4 × 3–1/2 × 1/4	139.7
8S10	22.3	W12 × 58	W8 × 21	L6 × 3–1/2 × 1/2	15.24	5.08	8.89	2L4 × 3–1/2 × 1/4	139.7

such as top and web angle dimensions and bolt spacing on connection behavior. The test setup includes two beams segments with equal lengths which are symmetrically bolted to a stub column. Beam ends are simply supported and a stub column can move vertically and applied load on center of the stub column creates moment in the connection. Fig. 1 shows the test setup configuration for 14SX specimens. The other connections configurations (8SX) are similar to 14SX models with different beam and column sections which are listed in Table 1. These specimens have two rows of bolts in web angles.

2.1. Geometry of connection models

Azizinamini's experiments include 18 test specimens of bolted top and seat angle connections with web angles. Geometrical properties of the specimens are listed in Table 1. Specimen 14S3 is similar to 8SX specimens and has two rows of bolts in web angles at 3 inch spacing [4].

2.2. Finite element modeling

ANSYS [22] multi-purpose finite element modeling code is used to perform numerical modeling of connections. FE models were created using ANSYS Parametric Design Language (APDL). Geometrical and mechanical properties of connection models were used as the parameters, thus the time used for creating new models is considerably reduced.

Numerical modeling of connections is done including the following considerations: all components of connections such as beam, column, angles and bolt's head are modeled using eight node first order SOLID45 elements and bolt shanks are modeled using SOLID64 element which can consider the thermal gradient used to apply pretensioning force on bolts. [22, 23] Bolt holes are 1.6 mm larger than bolt diameter. Just half

of the connection is modeled because of the symmetry that exists about the web plane. The model contains just flange and stiffeners of the column, because of the high rigidity of the column as a result of its stiffeners.

ANSYS can model contact problems using contact pair elements: CONTA174 and TARGE170, which pair together in a way such that no penetration occurs during loading process. So the interaction between adjacent surfaces, including angle–beam flange, bolt head–nut, bolt hole–bolt shank and also the effect of friction were modeled using the mentioned contact elements. Bolt head and nut were modeled hexagonally and similar to the actual shape. To consider the frictional forces, Coulomb's coefficient is assumed to be 0.25, since it yielded results in better agreement with test results. In Refs. [8,9], the value of 0.1 was considered for the friction coefficient, which is one-third of the usual value of 0.33 proposed in the literature for class "A" type steel surfaces [3]. Fig. 2 shows the FE model and mesh pattern of connection. The shape of the bolt head and the nut, the stiffeners of column stub and the nonlinearity of bolt shanks (discussed in the following Section 2.4) are the main differences between the current study and the study conducted by Citipitioglu et al. [7].

2.3. Boundary conditions and loading

To satisfy the symmetry requirements, all nodes of the web plane are restrained against outward motion. It should be noted that, since the beams of the connections are compact sections, the local buckling instabilities occur in the inelastic range or high stress levels. The von Mises stress distribution in FE models clarifies that the beam remains almost elastic and so the local buckling failure mode can be ignored in the FE models.

Bolt pretensioning force is applied as the first load case by a thermal gradient which is applied on bolt shanks to create

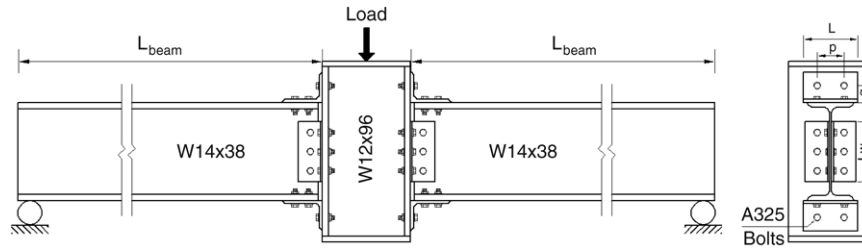


Fig. 1. Test setup configuration and the connection parameters of specimens 14SX [4].

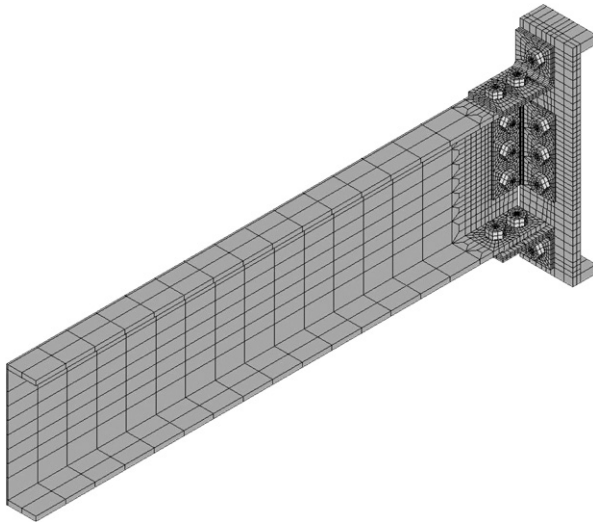


Fig. 2. FE modeling of connection 14S2 by 16070 elements and 17134 nodes.

an equivalent pretensioning force. Since in this experiment there is no information about the value of bolt pretensioning force, design values of pretensioning force [3] were applied. 178 kN pretensioning force is applied to 22.3 mm bolt diameter and 133 kN for 19.1 mm bolt diameter. A 50 mm vertical displacement is applied on the nodes of the beam end to impose the moment on connection. This value of beam end displacement yields a rotation close to 0.03 rad. The resulting moment and relative rotation of connections are evaluated respectively by Eqs. (1) and (2):

$$M = P \cdot L \quad (1)$$

$$R = \frac{\varepsilon_1 - \varepsilon_2}{h}, \quad (2)$$

where M is the applied connection moment, P is the summation of the reaction forces of applied displacement on beam end nodes; L corresponds to beam length, R is relative rotation of connection, h is beam depth, ε_1 and ε_2 are relatively top and bottom flange horizontal displacements.

2.4. Material properties

Stress–strain relation for all connection components, except bolts, is represented using three-linear constitutive model. An isotropic hardening rule with von Mises yielding criterion is used to simulate plastic deformations of connection components and fracture of material is not considered. ASTM A36 steel was used for the beam, column and angles. In

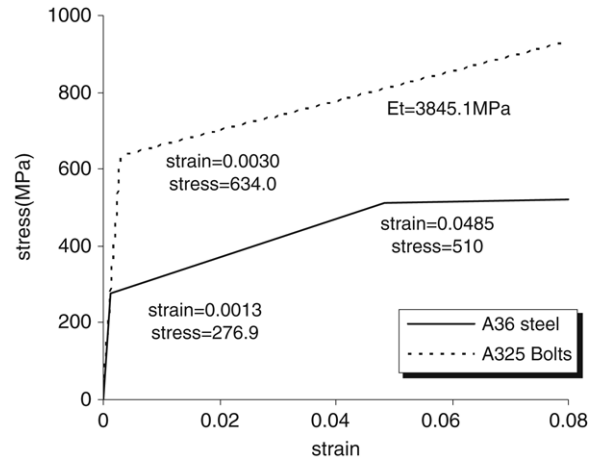


Fig. 3. Material properties of beam, column and angle [4].

the current study, mechanical properties of beam, column and angles are taken from a numerical study conducted by Citipitioglu et al. [7]. Yield stress and ultimate strength of bolts are assumed based on nominal properties of A325 bolts. Bolt materials were modeled as bilinear with 634.3 MPa yield stress and ultimate stress of 930 MPa at 8% strain. Modulus of elasticity and Poisson’s ratio is considered respectively as 210 GPa and 0.3. Fig. 3 shows the stress–strain relation of A36 steel used for beam and angle material in the current study.

3. Verification of finite element models

Since there is no valid test result for this type of connections under a combination of shear and moment or even pure shear force, the applicability of the method is studied for the case of connections subjected to moment only.

To evaluate the accuracy of the finite element modeling approach, 17 FE models are created according to Azizinamini tests and the results are compared with test results. Figs. 4 and 5 show the deformed shape of connection. Fig. 6 shows a comparison between moment–rotation relations of FE modeling and test data. As it can be seen from these figures, results obtained by finite element models have a good agreement with test data and the numerical study of Refs. [4,16]. Difference between numerical simulation and test results may be due to several causes, like numerical modeling simplification, test specimen defects, residual stress and bolt pretension.

The difference between test data and numerical models grows in the nonlinear portion of the curves. A major cause

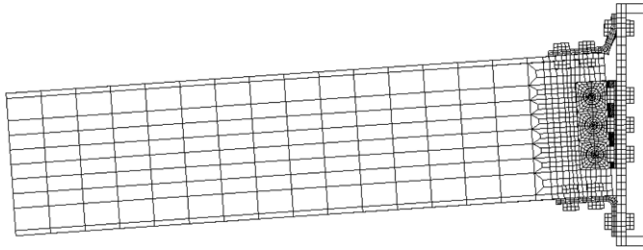


Fig. 4. Deformed shape of connection 14S2 at 0.03 rad, Scaled by 2.

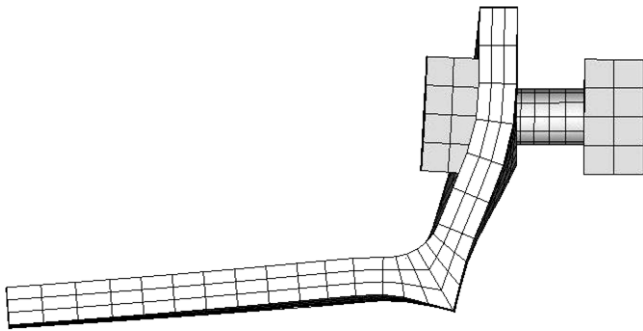


Fig. 5. Top bolt–angle surfaces interaction of connection 14S2 at 0.03 rad, Scaled by 2.

is the nonlinear constitutive laws for materials, especially for situations where only uniaxial values of the stress–strain curves are available [24].

As can be seen from Fig. 6, in specimens 8S3 and 8S4 the difference between finite element modeling and test data is higher than for other specimens while the two finite element results (current study and Citipitioglu study) have a good agreement. This difference is most likely due to test specimen defects like geometrical measuring or bolt pretensions.

4. Effect of shear force on connection behavior

4.1. Moment–rotation properties of specimens

To study the influence of shear force on moment–rotation behavior of bolted angle connections with web angles, specimens 14S2 and 14S2W10 are subjected to four different levels of shear force. Connection 14S2 is defined in Table 1. Connection 14S2W10 is created using parametric model of specimen 8SX, so it is the same as the 14S2, and the only difference is that it has two web angle bolts and 100 mm of web angle length. The data of previous studies conducted in [21] is added to results of the current study. So the new formulation is obtained based on the results of 31 models.

Since there are many configurations for bolted angle connections with different parameters (such as bolt diameter, angles thickness, surfaces conditions, material properties and so on), to have a better understanding of the results and a fair data processing, the results are converted to dimensionless values using a reference shear value, initial rotational stiffness for the case of zero shear force and web angle shear capacity defined below.

General properties of models are listed in Table 2. The first 23 models of Table 2 are the results of a previous study [21] and the rests are for specimens 14S2 and 14S2W10.

The first column of Table 2 is the specimen numbers. The second column is the type of connection which was defined earlier in Table 1. The titles of the other columns are defined as follows:

Reference moment (M_R): the corresponding moment at the intersection point of tangent lines in the linear and full nonlinear regions presented in Fig. 7. Since the connection moves gradually into the nonlinear range, the parameter M_R is defined as cited, to be calculated more reliable.

Reference shear (S_R): The corresponding shear value of reference moment would be computed by Eq. (3) as follows:

$$S_R = \frac{M_R}{L_{\text{beam}}} \quad (3)$$

L_{beam} is the beam length (1.5 m in current study).

Applied shear force (S_C): applied shear force on tip of the beam which is twice the applied shear force on FE models because of symmetry existing in finite element model connections. Positions of applied loads are shown in Fig. 8. The applied shear force is raised from zero up to the connection's ultimate capacity where convergence difficulties in the last step of loading (the monotonic moment loading) appear. In Fig. 9, moment–rotation behavior of the 8S1 and 14S2 models which were subjected to combined shear and moment loading is shown. It can be seen that, because of the shear force, a considerable reduction of initial rotational stiffness obtained while the shear force do not affect connection moment-resisting considerably.

Initial stiffness (K_i): K_i is the initial stiffness of connection in the case of zero shear force and/or the slope of the linear part of the moment–rotation curve. In the literature, methods have been proposed to determine the connection rotational stiffness [12, 13,16].

Reduced stiffness (K_r): K_r is the reduced initial rotational stiffness of connection under shear force, or the slope of the linear part of the moment–rotation curve, where it is subjected to a combination of shear force and bending moment.

Normalized shear (S_n): S_n is the normalized shear force which can be computed by Eq. (4) as follows:

$$S_n = \frac{S_C}{S_R} \quad (4)$$

Normalized stiffness ($R_{\text{stiffness}}$): normalized stiffness parameter is the ratio of reduced stiffness divided by the initial stiffness and is computed by Eq. (5)

$$R_{\text{stiffness}} = \frac{K_r}{K_i} \quad (5)$$

4.2. Data processing

In Ref. [21], the normalized shear force of connections was plotted against normalized stiffness, and then a second order curve was fitted to data (Eq. (6)). In the current study the effect

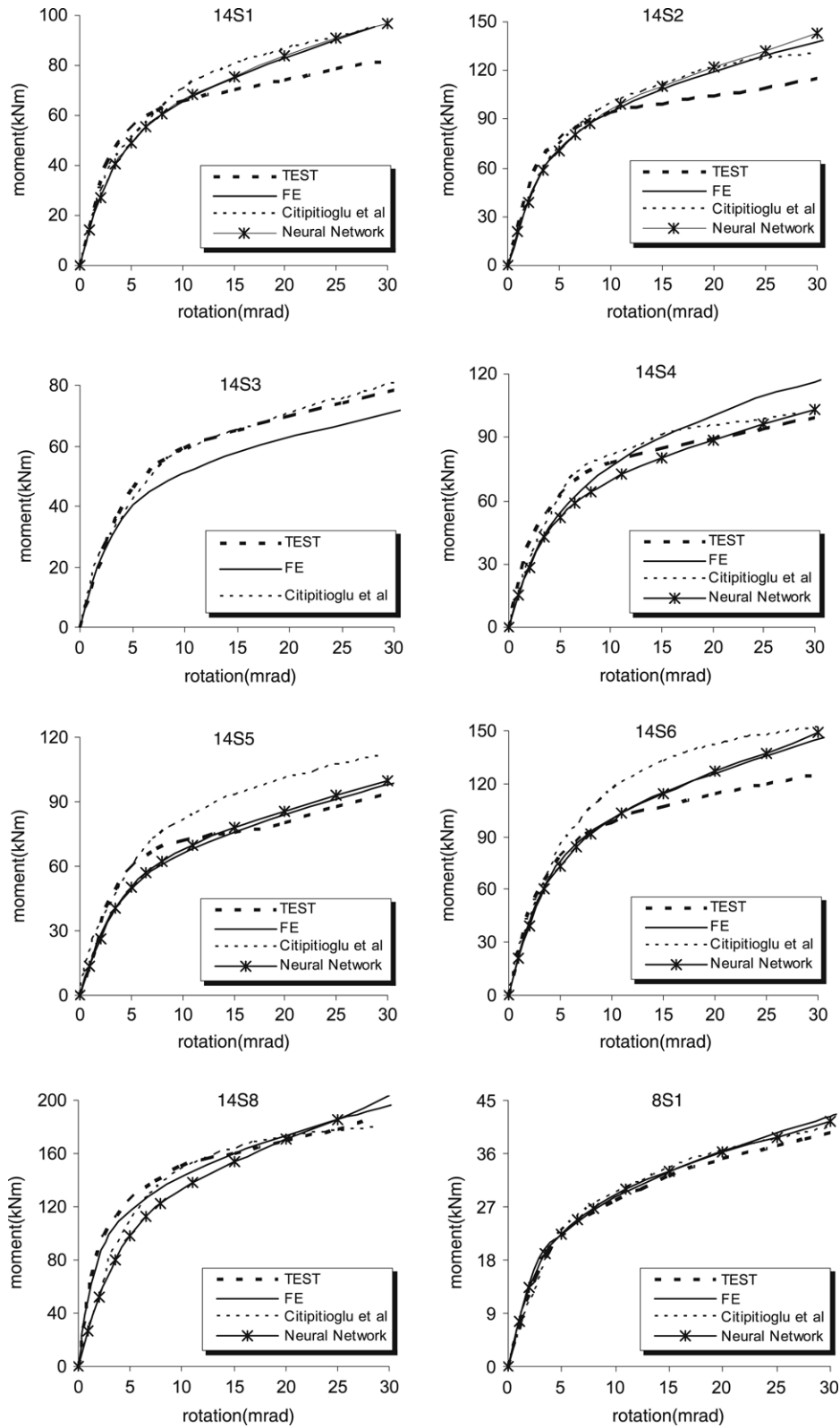


Fig. 6. Comparison between the results of FE models and experiments of Azizinamini [6].

of web angle yield shear capacity is taken into account which is computed by Eq. (7).

$$R_{\text{stiffness}} = -0.0031S_n^2 + 0.008S_n + 0.98 \quad (\text{F. Danesh et al.}) \quad (6)$$

$$W_y = 2(L_w \cdot t_w \cdot F_y). \quad (7)$$

In Eq. (7), L_w is the web angle length, t_w is the thickness of web angle and F_y refers to the yield stress of web angle

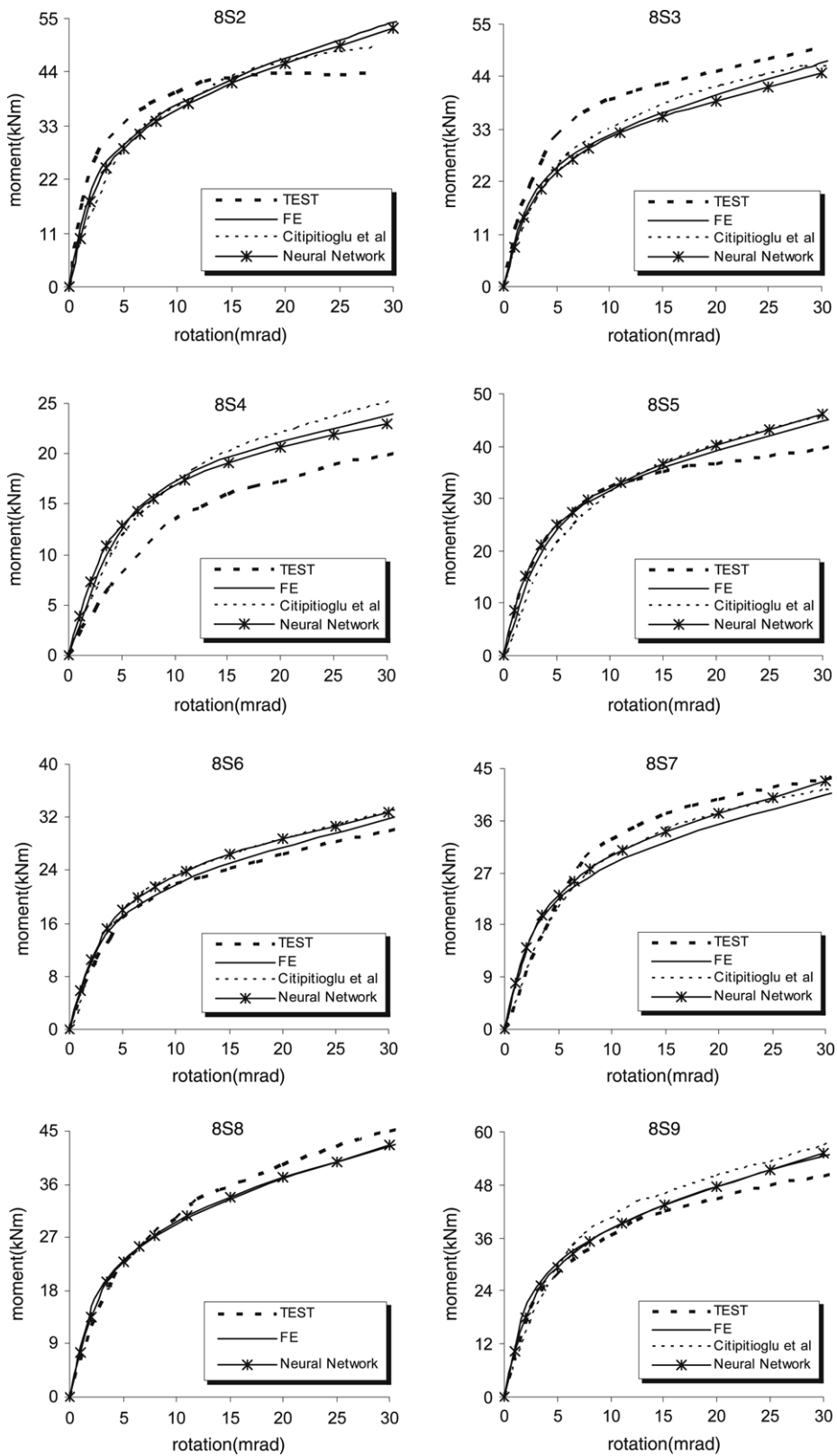


Fig. 6. (continued)

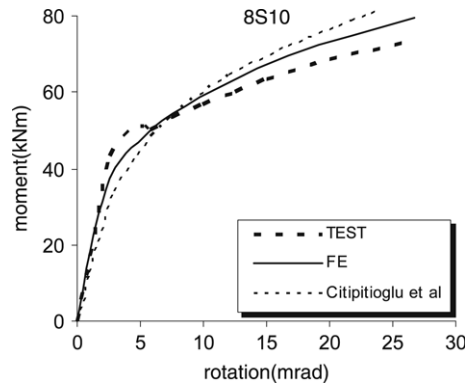


Fig. 6. (continued)

Table 2
Moment–rotation properties of specimens under shear force

Number	Specimen	Reference moment (kN m)	Reference shear (kN)	Applied shear force (kN)	Initial stiffness (kN m/mrad)	Reduced stiffness (kN m/mrad)	Normalized shear (S_n)	Normalized stiffness ($R_{stiffness}$)
1	14S1	62.46	41.64	0.00	13.77	13.77	0.00	1.00
2	14S1	62.46	41.64	280	13.77	13.26	6.72	0.96
3	14S1	62.46	41.64	350	13.77	12.57	8.41	0.91
4	14S1	62.46	41.64	500	13.77	10.65	12.00	0.77
5	14S8	134	89.3	170	27.06	26.96	1.9	0.996
6	14S8	134	89.3	200	27.06	26.25	2.24	0.97
7	14S8	134	89.3	300	27.06	24.18	3.36	0.89
8	14S8	134	89.3	400	27.06	23.68	4.48	0.87
9	8S1	39.45	26.3	80	7.58	7.39	3.04	0.975
10	8S1	39.45	26.3	131.6	7.58	7.31	5.00	0.96
11	8S1	39.45	26.3	200	7.58	7.00	7.6	0.947
12	8S1	39.45	26.3	240	7.58	6.05	9.11	0.798
13	8S1	39.45	26.3	280	7.58	5.23	10.26	0.69
14	8S1	39.45	26.3	300	7.58	3.86	11.4	0.51
15	8S5	31.35	20.9	20	6.67	6.65	0.957	0.997
16	8S5	31.35	20.9	146.6	6.67	6.352	7.01	0.947
17	8S5	31.35	20.9	200	6.67	5.746	9.57	0.861
18	8S5	31.35	20.9	230	6.67	5.531	11	0.83
19	14S3	51.3	34.2	56	19.84	18.53	1.64	0.934
20	14S3	51.3	34.2	120	19.84	18.22	3.5	0.92
21	14S3	51.3	34.2	210	19.84	16.64	6.14	0.84
22	14S3	51.3	34.2	300	19.84	14.35	8.77	0.723
23	14S3	51.3	34.2	410	19.84	9.045	12	0.456
24	14S2	90.35	60.2	0.00	39.68	39.68	0.00	1.00
25	14S2	90.35	60.2	162	39.68	36.47	2.69	0.92
26	14S2	90.35	60.2	300	39.68	32.35	5.00	0.81
27	14S2	90.35	60.2	486	39.68	26.18	8.07	0.66
28	14S2W10	87.51	58.3	0.00	35.79	35.79	0.00	1.00
29	14S2W10	87.51	58.3	84	35.79	33.59	1.44	0.85
30	14S2W10	87.51	58.3	150	35.79	32.35	2.57	0.90
31	14S2W10	87.51	58.3	210	35.79	27.13	3.60	0.76

materials. It should be noted that the real shear capacity of a connection is $1/\sqrt{3}$ times W_y and the W_y is used just for normalizing. For this purpose, the value of S_n is scaled for all specimens by dividing it by W_y/S_r .

Von Mises stress distribution in the connection angles under shear force (second load case) is presented in Fig. 10. Relatively high levels of stress in the web angles due to shear force may be a rational reason for the relation between the connection initial stiffness and the shear capacity of the web angles.

Fig. 11 shows the plots of scaled S_n against $R_{stiffness}$ and its second order polynomial curve fitting.

The accuracy of regressions was very good and a value of $R^2 > 0.9$ was observed for almost all the specimens. The equations and values of R^2 are listed in Table 3. As cited in Section 4.1, there are alternative configurations for bolted angle connections and so the equations in Table 3 are obtained for each connection separately while a general equation is needed. In Table 3 the coefficient of S_n^2 in the fitted equations

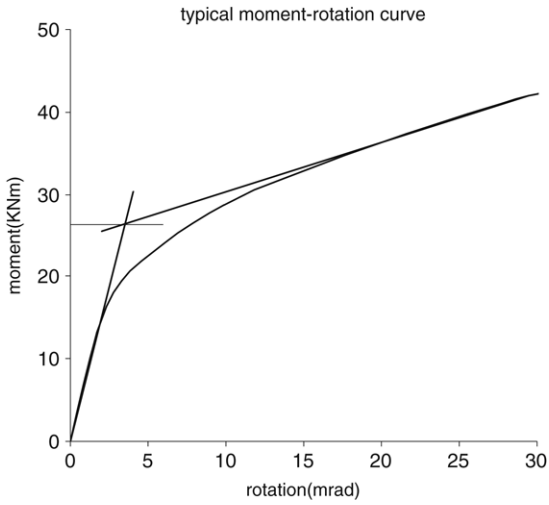


Fig. 7. Typical moment–rotation curve of connection and its reference moment.

is almost (1/24) of (W_y/S_R) . Ignoring the second term of these equations, the simplified general equation (8) is proposed.

$$R_{stiff} = 1 - \left(\frac{W_y}{24S_R} \right) \left(\frac{S_n S_R}{W_y} \right)^2. \quad (8)$$

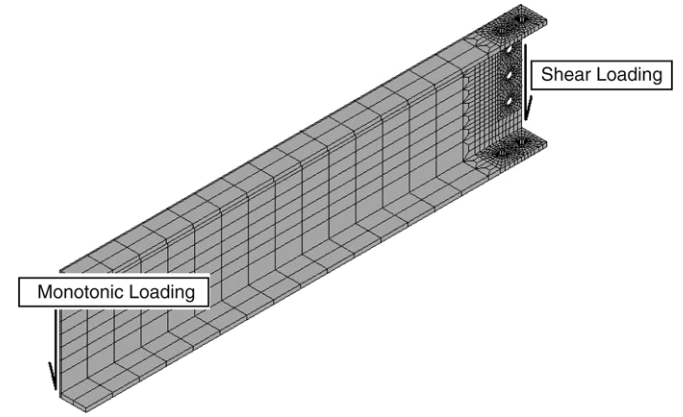


Fig. 8. Location of applied shear force and monotonic loading.

This gives Eq. (9) as follows:

$$R_{stiff} = 1 - \left(\frac{S_R}{24W_y} \right) S_n^2. \quad (9)$$

In Table 4 the accuracy of the proposed formulation is compared with the equation proposed in Ref. [21]. This comparison reveals that considering web angle shear capacity

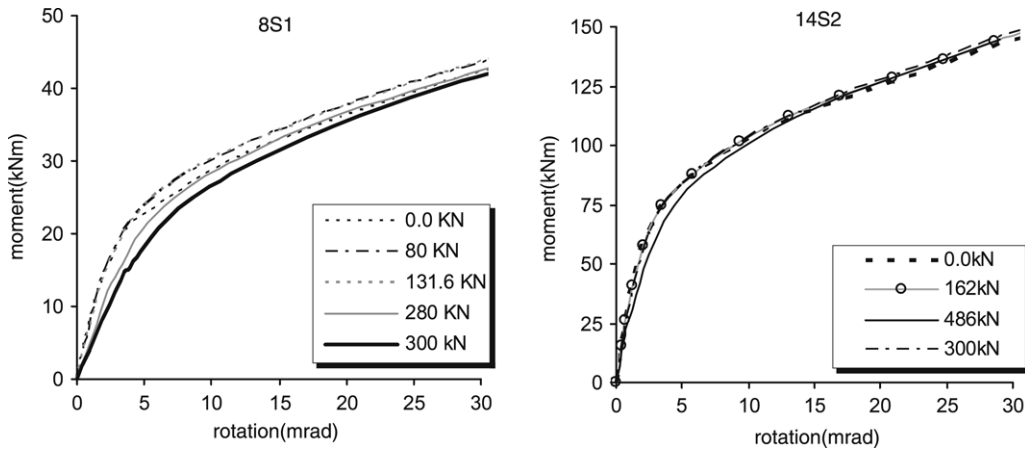


Fig. 9. Moment–rotation behavior of 8S1 and 14S2 specimens under combined shear and moment loading.

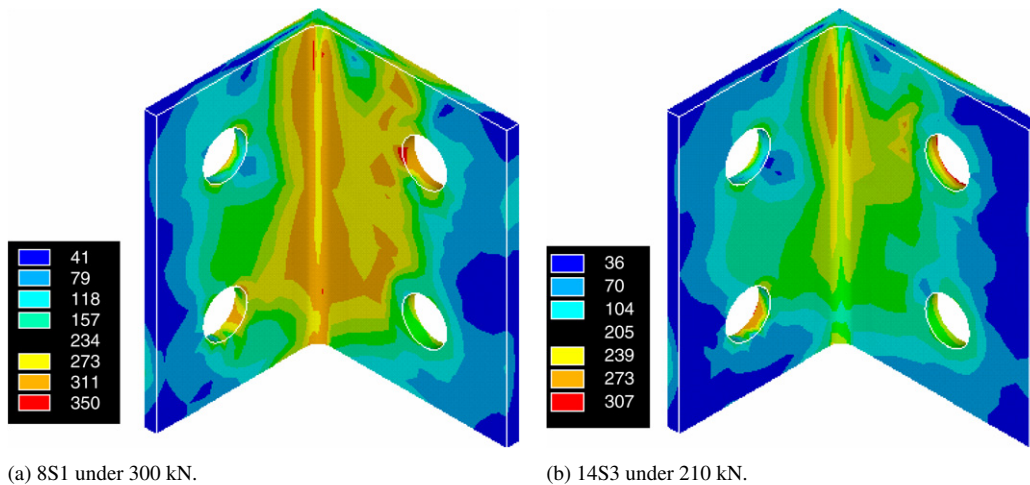


Fig. 10. Von Mises stress distribution in the web angles of connection.

Table 3
Regression equations for each specimen

Specimen	Reference shear (kN)	Web angle length (mm)	Web angle thickness (mm)	$W_y = 2^*(L_w \cdot t_w \cdot F_y)$ (kN)	W_y/S_R	Regression equation	R^2
14S1	41.64	215.9	6.35	744.6	17.88	$y = -0.7443x^2 + 0.174x + 0.9946$	0.99
14S2	60.20	215.9	6.35	744.6	12.37	$y = -0.2721x^2 - 0.3494x + 1.0021$	0.999
14S2W10	58.3	100	6.35	338.5	5.81	$y = -0.5829x^2 - 0.0052x + 0.9952$	0.97
14S3	34.2	139.7	6.35	481.8	14.09	$y = -0.67x^2 - 0.0266x + 0.976$	0.99
14S8	89.3	215.9	6.35	744.6	8.34	$y = -0.456x^2 - 0.0211x + 1.0054$	0.89
8S1	26.3	139.7	6.35	481.8	18.32	$y = -2.2311x^2 + 0.7225x + 0.9687$	0.94
8S5	20.9	139.7	6.35	481.8	23.05	$y = -0.9856x^2 + 0.1182x + 0.9935$	0.98

Table 4
Accuracy of the proposed equation

No.	Specimen	S_n	S_R	W_y	$R_{stiffness}$ (from FE)	$R_{stiffness}$ (from Eq. (8))	Error 1 (%)	$R_{stiffness}$ (Danesh et al.)	Error 2 (%)
1	14S1	0	41.64	744.6	1	1	0	0.98	2.00
2	14S1	6.72	41.64	744.6	0.96	0.90	6.25	0.90	6.25
3	14S1	8.41	41.64	744.6	0.91	0.84	7.69	0.84	7.69
4	14S1	12	41.64	744.6	0.77	0.67	12.99	0.64	16.88
5	14S8	1.9	89.3	744.6	1.00	0.97	3.00	0.98	2.00
6	14S8	2.24	89.3	744.6	0.97	0.96	1.03	0.98	-1.03
7	14S8	3.36	89.3	744.6	0.89	0.90	-1.12	0.97	-8.99
8	14S8	4.48	89.3	744.6	0.87	0.83	4.60	0.96	-10.34
9	8S1	3.04	26.3	481.8	0.98	0.98	0.00	0.98	0.00
10	8S1	5	26.3	481.8	0.96	0.94	2.08	0.95	1.04
11	8S1	7.6	26.3	481.8	0.95	0.85	10.53	0.87	8.42
12	8S1	9.11	26.3	481.8	0.80	0.79	1.25	0.80	0.00
13	8S1	10.26	26.3	481.8	0.69	0.73	-5.80	0.75	-8.70
14	8S1	11.4	26.3	481.8	0.51	0.67	-31.37	0.68	-33.33
15	8S5	0.957	20.9	481.8	1.00	1.00	0.00	0.98	2.00
16	8S5	7.01	20.9	481.8	0.95	0.90	5.26	0.89	6.32
17	8S5	9.57	20.9	481.8	0.86	0.82	4.65	0.78	9.30
18	8S5	11	20.9	481.8	0.83	0.76	8.43	0.71	14.46
19	14S3	1.64	34.2	481.8	0.93	0.99	-6.45	0.99	-6.45
20	14S3	3.5	34.2	481.8	0.92	0.96	-4.35	0.97	-5.43
21	14S3	6.14	34.2	481.8	0.84	0.88	-4.76	0.92	-9.52
22	14S3	8.77	34.2	481.8	0.72	0.75	-4.17	0.82	-13.89
23	14S3	12	34.2	481.8	0.46	0.52	-13.04	0.64	-39.13
24	14S2	0	60.2	744.6	1.00	1.00	0.00	0.98	2.00
25	14S2	2.69	60.20	744.60	0.92	0.98	-6.05	0.98	-6.05
26	14S2	5.00	60.20	744.60	0.81	0.91	-13.38	0.94	-14.10
27	14S2	8.07	60.20	744.60	0.66	0.70	-6.44	0.84	-27.68
28	14S2W10	0.00	58.30	338.50	1.00	1.00	0.00	0.98	2.00
29	14S2W10	1.44	58.30	338.50	0.94	0.99	-4.89	0.99	-4.79
30	14S2W10	2.57	58.30	338.50	0.90	0.95	-5.84	0.98	-8.90
31	14S2W10	3.60	58.30	338.50	0.76	0.91	-19.74	0.97	-27.63

in calculating the stiffness reduction of connection due to shear load gives more accurate results, especially for large values of shear forces. For example, Eq. (6) gives a -39.13% error for specimen 14S3 under 410 kN shear force but the estimated value by Eq. (9) has just -24.8% error. According to the information of Table 4, both proposed equations have high errors when large magnitudes of shear force exist.

4.3. Step by step implementation of the method

1. Calculating connection initial rotational stiffness, K_i and reference moment M_R using available moment-rotation curve or compute it directly using other proposed methods

and dividing it by beam length (Eq. (3)) to obtain reference shear (S_R).

2. Computing S_n by dividing the applied shear force by reference shear force. (Eq. (4)).
3. Using web angle dimensions and yield stress (Eq. (7)) of web angle material to calculate W_y .
4. Put the values of S_R , S_n and W_y in Eq. (9) to calculate the reduction factor of initial rotational stiffness.

5. Conclusion

In this paper, the influence of web angle on shear load capacity and initial rotational capacity of top and seat angle connections with double web angles is studied. The FE method

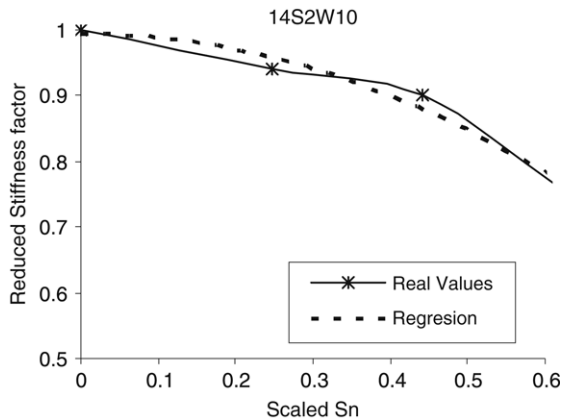


Fig. 11. Curve fitting for connection 14S2W10.

is used in this study and several FE models were created and verified by earlier numerical and experimental studies. Comparison of results showed a good accuracy for finite element simulation. The probability of local buckling of the beam is discussed and according to the stress distribution pattern on beam and section compactness, it was found that such instabilities will not occur. The deteriorative effect of shear force on connection initial rotational stiffness is studied. Shear force applies to present the gravitational load reactions at the beam end after the pre-tensioning load case, and then the monotonic moment loading was applied on the beam end. Moment–rotation curves of connections are derived and the change rate of rotational stiffness and its sensitivity to web angle dimensions is studied. It was cleared that considering web angle shear capacity gives more accurate results. Based on the results of 31 FE models, a second order formula is proposed to estimate the deterioration of connection rotational stiffness due to shear force. The accuracy of the method is compared with the study conducted by Danesh et al. which showed a better estimation of the proposed formula in current study.

The follow may be investigated further to improve the proposed method:

- Effect of bolt diameter, bolt pretension, friction coefficient and seat angle dimensions may be studied on connection behavior under shear force.
- Changes in yield moment and nonlinear stiffness of connection and their sensitivity under combination of shear force could be evaluated precisely.

Acknowledgments

With special thanks to Mr. Tafazzoli (Eng) for his kind help and Professor Shiro Takada for providing the opportunity of using his software on this article.

References

- [1] Mahin SA. Lessons from damage to steel buildings during the Northridge

- earthquake. *Engineering Structures* 1998;20:261–70.
- [2] Akiyama Hiroshi. Evaluation of fractural mode of failure in steel structures following Kobe lessons. *Journal of Constructional Steel Research* 2000;55:211–27.
- [3] AISC. *Manual of steel construction—Load and resistance factor design*. Chicago (IL): American Institute of Steel Construction; 1995.
- [4] Akbas Bulent, Shen Jay. Seismic behavior of steel buildings with combined rigid and semi-rigid frames. *Turkish Journal of Engineering and Environmental Sciences* 2003;27:253–64.
- [5] Azizinamini A. Monotonic response of semi-rigid steel beam to column connections. M.S. thesis. Columbia: University of South Carolina; 1982.
- [6] Shen J, Astaneh-Asl A. Hysteretic behavior of bolted-angle connections. *Journal of Constructional Steel Research* 1999;51:201–18.
- [7] Citipitioglu AM, Haj-Ali RM, White DW. Refined 3D finite element modeling of partially restrained connections including slip. *Journal of Constructional Steel Research* 2002;8:995–1013.
- [8] Kishi N, Ahmed A, Yabuki N. Nonlinear finite element analyses of top and seat-angle with double web-angle connections. *Journal of Structural Engineering and Mechanics* 2001;12:201–14.
- [9] Ahmed A, Kishi N, Matsuoka K, Komuro M. Nonlinear analysis on prying of top- and seat-angle connections. *Journal of Applied Mechanics* 2001; 4:227–36.
- [10] Pirmoz A. Evaluation of nonlinear behavior of bolted connections under dynamic loads. M.S. thesis. Tehran (Iran): K.N.Toosi University; 2006.
- [11] Danesh F, Pirmoz A. 3D finite element modeling of bolted angle connections. In: 9th Canadian conference on earthquake engineering. Paper number 1024.
- [12] Shen J, Astaneh-Asl A. Hysteretic model of bolted-angle connections. *Journal of Constructional Steel Research* 2000;54:317–43.
- [13] Danesh F. Nonlinear dynamic analyses of semi-rigid steel frames and comparison with test results. In: Third international conference of seismology and earthquake engineering. 1999.
- [14] Abdala KM, Stavroulakis GEA. Backpropagation neural network model for semi-rigid joints. *Microcomputers in Engineering* 1995; 77–87.
- [15] De Lima LRO, Vellasco PCG da S, de Andrade SAL, da Silva JGS. Neural networks assessment of beam-to-column joints. *Journal of the Brazil Society of Mechanical Science & Engineering* 2005;314–24.
- [16] Pirmoz A, Gholizadeh S. Predicting of moment–rotation behavior of bolted connections using neural networks. In: 3rd national congress on civil engineering. 2007. Paper number 2108A.
- [17] Okazaki T, Engelhard MD, Nakashima M, Suita K. Experimental study on link-to-column connections in steel eccentrically braced frames. In: 13th world conference on earthquake engineering. 2004. Paper no. 275.
- [18] Yang J-G, Murray TM, Plaut RH. Three-dimensional finite element analyses of double angle connections under tension and shear. *Journal of Constructional Steel Research* 2000;54:227–44.
- [19] Hong K, Yang JG, Lee SK. Parametric study of double angle framing connections subjected to shear and tension. *Journal of Constructional Steel Research* 2001;57:997–1013.
- [20] Hong K, Yang JG, Lee SK. Moment–rotation behavior of double angle connections subjected to shear load. *Engineering Structures* 2002;24: 125–32.
- [21] Danesh F, Pirmoz A, Saedi Daryan A. Effect of shear force on initial stiffness of top and seat angle connections with double web angles. 2007; 63(9): 1208–18.
- [22] ANSYS User's manual, version 6.1.
- [23] Belytschko T, Liu WK, Moran B. *Nonlinear finite elements for continua and structures*, vol. 54. John Wiley & Sons Ltd. 650P. 2000; 2001. p. 317–43.
- [24] Maggi YI, Goncalves RM, Leon RT, Ribeiro LFL. Parametric analyses of steel bolted end plate connections using finite element modeling. *Journal of Constructional Steel Research* 2005;61:689–708.